Supplementary Material

Biophysical Characterization of Mutants of *Bacillus subtilis* Lipase Evolved for Thermostability: Factors Contributing to Increased Activity Retention

Characterization of recovered LipA variant XI

NMR experiments showed close conformational similarity of thermally treated LipA variant XI to the native protein. Thermal inactivation profiles were recorded for further characterization of the recovered protein. The profiles revealed significant differences (Fig. S1). Importantly, protein subjected to thermal denaturation and re-folding at either 60 or 80 °C retains more activity after the heating and cooling process than native variant XI.

To prove that indeed active site residues are responsible for the activity retention of variant XI, control experiments were carried out using appropriate LipA mutants, specifically those having mutations at the active site residues (S77C, D133N and H156L).

Construction of the appropriate clones

An expression clone of variant XI cloned into pET-22b (+) was obtained in a previous study[S1]. This construct was subjected to site-directed mutagenesis to obtain S77C, D133N and H156L mutants. PCR and DNA preparation/sequencing were performed as described for construct preparation (see Methods in the main text).

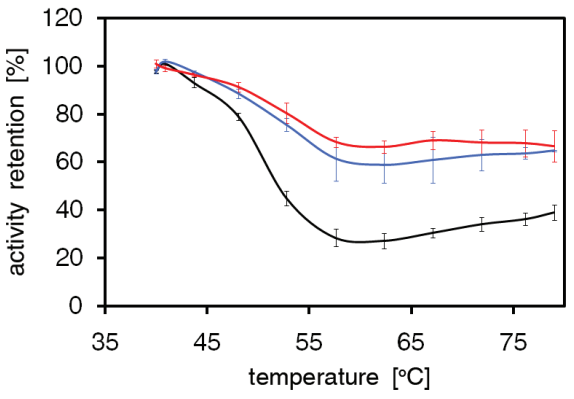

Figure S1. Thermal inactivation profiles of ^{15}N-labeled LipA variant XI. Native protein is represented by the black curve, protein treated at 60 °C by the blue curve and enzyme treated at 80 °C is represented by the red curve.

The following primers were used: for S77C mutation: 5'-TATTGTCGCTCACTGCATGGGGGGCGC-3', antisense 5'-GCGCCCCCCATGCAGTGAGCGACAATA-3'; for D133N mutation: 5'-CACATCCATTTACAGCAGTGCCAATGATATTGTCATGAATTGTTTA-3', anti-sense: 5'-TAAACAATTCATGACAATATCATTGGCACTGCTGTAAATGGATGTG-3'; and for H156L mutation: 5'-CCATGGCGTTGGACTCATGGGCCTTCTGT-3', anti-sense: 5'-ACAGAAGGCCCATGAGTCCAACGCCATGG-3'.

Preparation of crude protein

E. coli BL21 (DE3) electrocompetent cells were transformed, transformants were selected and inoculated into 20 mL of ZYP-505 medium with carbenicillin[S2]. The culture was grown at 30 °C, 150 rpm shaking for 24 h using an Infors HT Ecotron shaker. 20 µL of this pre-culture were inoculated into 20 mL of ZYP-5052 autoinducing expression medium with carbenicillin. This system exports expressed protein to the periplasm, therefore the target protein is finally present in the supernatant. The culture was grown at 37 °C, 150 rpm shaking for 24 h. The cells were spun (10000 x g, 10 min., 4 °C) and the supernatant was diluted 4–fold using water; this solution was used in the study on inactive variant XI. Protein expression was analyzed using SDS-PAGE.

Results

Unfortunately, only the S77C mutant could be expressed efficiently. Thermal inactivation profiles were recorded for the inactive mutant S77C and for the active variant XI as a reference. The S77C mutant exhibited no lipase activity before thermal treatment, nor did any activity appear after heating. Therefore, it was concluded that the native active site is responsible for activity retention after thermal treatment, which is consistent with results obtained using NMR.

Thermal inactivation profiles at various conditions

Thermal inactivation profiles of the LipA variants were determined at a variety of conditions. While part of the

data is shown in the main article (Fig. 1), remaining profiles are presented in Fig. S2. Besides following the trends described in the Results and Discussion, these profiles provide additional information.

Irreversible activity loss of all the enzyme variants was observed at pH 12 (Fig. S2B) and in ethylene glycol above 75 °C (Fig. S2D). This illustrates the relevance of ionic and hydrophobic interactions in the enzyme re-constitution process. The LipA tertiary structure is much less stable at pH 12 than at neutral pH, as it was confirmed using CD melting experiments. Oppositely, ethylene glycol seems to enable re-folding from early unfolded intermediates of wild-type and variant X LipA, since the slopes are shifted by 3 to 8 °C towards

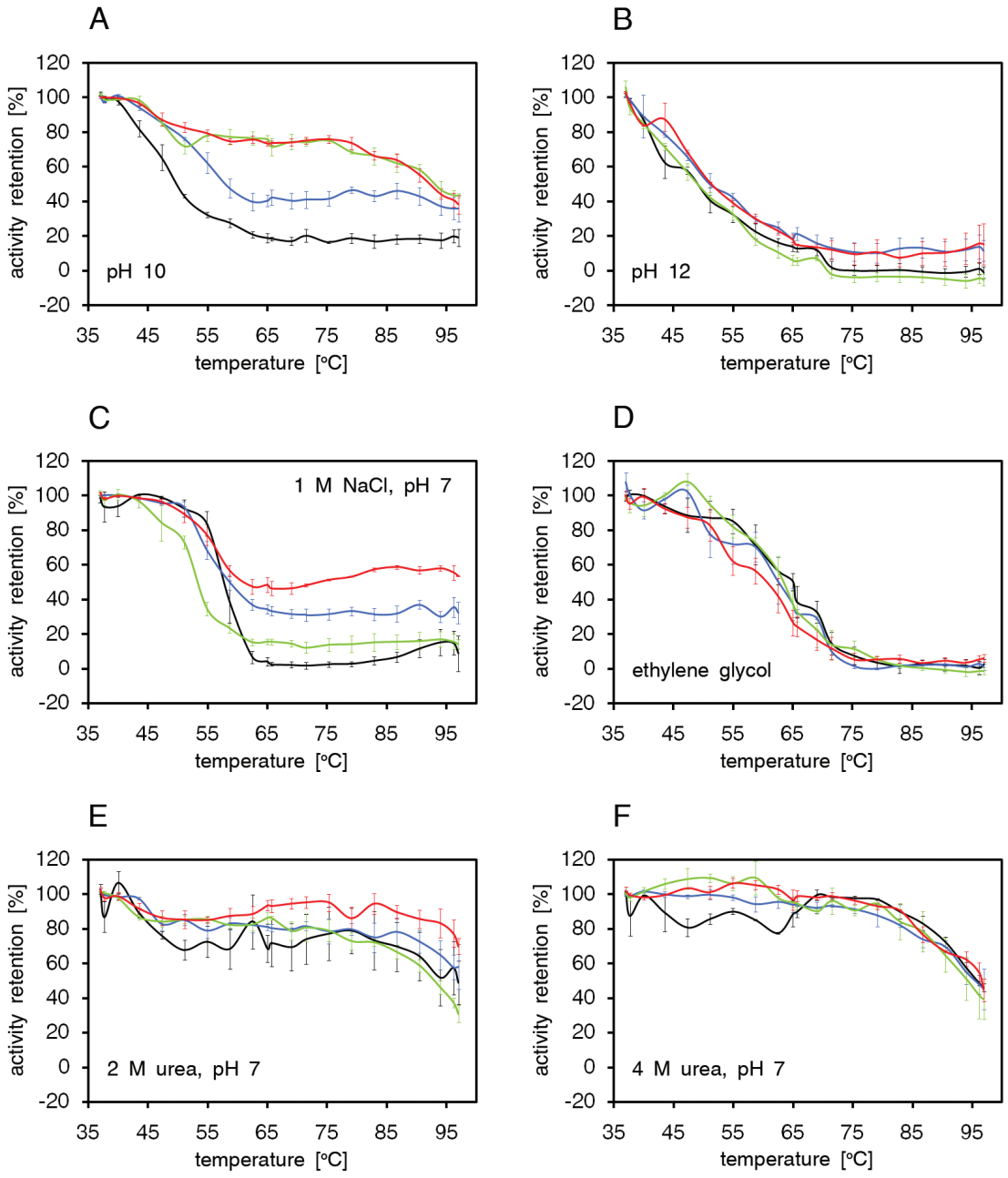

Figure S2. Thermal inactivation profiles of Lipase A variants determined at various conditions. Wild-type enzyme is represented by black lines, variant IX by blue lines, variant X by green lines and variant XI by red lines. Experiments were performed as described in Methods.

higher temperatures compared to experiments at neutral pH. Variant IX and XI slope positions do not seem to be significantly altered in ethylene glycol.

Furthermore, ionic interactions are able to differentiate protein variants, as can be seen in the experiments at pH 7 (Fig. 1A in main text), pH 10 (Fig. S2A) and in the presence of NaCl (Fig. S2C). Activity retention levels determined for denaturation above 75 °C are similar at pH 10 and 7 for all variants. However, at pH 10 intermediates present at 60 °C and 80 °C seem to reconstitute with equal efficiency.

The properties of LipA variants seem to be altered by the presence of a high amount of sodium chloride (Fig. S2C). First of all, the wild-type lipase profile seems to be shifted approximately 6 °C towards higher temperature. This suggests that salt facilitates the recovery of functional WT enzyme from early unfolding intermediates. Still, unfolding of this variant above 65 °C appears to be irreversible regardless of salt presence. Variant IX and XI profiles seem to be shifted approximately 2-3 °C towards higher temperature in the presence of salt; the shift is lower than that of the wild-type protein. Interestingly, a lower activity retention was observed after heating both mutants above 65 °C in the solution containing NaCl than in the low ionic strength solution. Finally, variant X retains a much lower activity when heated above 60 °C and re-folded from solution containing a high concentration of NaCl.

Overall, these results indicate the relevance of ionic interactions in the process of thermal denaturation and re-naturation of evolved LipA mutants. The exceptional properties of variant X might result from the fact that its pI is lower than for other mutants and/or from the critical role of residues 33 to 35 (which are different in the other variants).

Time dependence of variant XI Lipase A activity loss at 60 and 80 °C

The thermal inactivation profiles of LipA mutants at neutral pH indicate that more activity is recovered after exposure to 80 °C than to 60 °C. The effect of thermal treatment at various temperatures was proven as follows. LipA variant XI solution (0.8 to 1.4 µM) in 10 mM sodium phosphate, pH 7.0, 0.03% sodium azide was prepared. The solution was subjected to a heat treatment and the residual activity was determined in a similar manner to that described for thermal inactivation profile experiments; however, no temperature gradient was applied. Instead, the protein was thermally treated for 15 min. overall, but various durations of heating at 60 and 80 °C were applied. Both experiments where heating at 60 °C was followed by heating at 80 °C, and opposite (80 °C heating followed by application of 60 °C) were performed. Results are shown in Fig. S3.

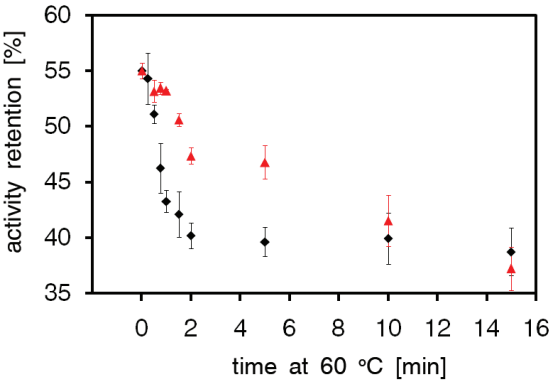

Figure S3. Variant XI Lipase A activity retention dependence on thermal treatment time at 60 °C and 80 °C. Enzyme was kept at 60 °C for the time specified on the horizontal axis, and at 80 °C for the remainder of time up to 15 min. Black diamonds represent experiments where heating at 60 °C was followed by treatment at 80 °C. Red triangles correspond to the experiment with an inverted thermal regime (80 °C followed by 60 °C).

The experiment shows that the longer the treatment at 60 °C, the more activity is lost. Interestingly, when lipase is first treated at 80 °C, the loss of activity at 60 °C occurs more slowly. This is in agreement with thermal inactivation profiles recorded for protein exposed to thermal denaturation before, which was used for NMR experiments (Fig. S1).

Lipase A denaturation observed by CD spectroscopy and fluorescence

Melting experiments record protein properties (for example CD ellipticity or also fluorescent dye binding) at the actual temperature. Fig. S4 shows example data recorded at neutral pH. Parameters describing LipA behavior were derived using this type of experiments.

The CD data was flanked by fluorescence studies using a dye binding to hydrophobic sites[S3]. The fluorescence melting experiments were performed as follows. Assay composition: 2.5 µL of 3.0 mg/mL Lipase A stock in 10 mM sodium phosphate, pH 7.0, 2.5 µL of SYPRO Orange Protein Gel Stain fluorescent dye (Sigma) diluted 20-fold using 10 mM sodium phosphate, pH 7.0, and 20 µL of appropriate buffer. Melting curves were recorded using a MyIQ Single Color Real-Time PCR Detection System (Biorad) using 0.5 °C steps with rate of 3 °C/min from 15 to 95 °C. The dye was excited at 545 nm and the emission was measured at 585 nm. The melting temperature was derived from plots of the derivative of the fluorescence intensity versus temperature.

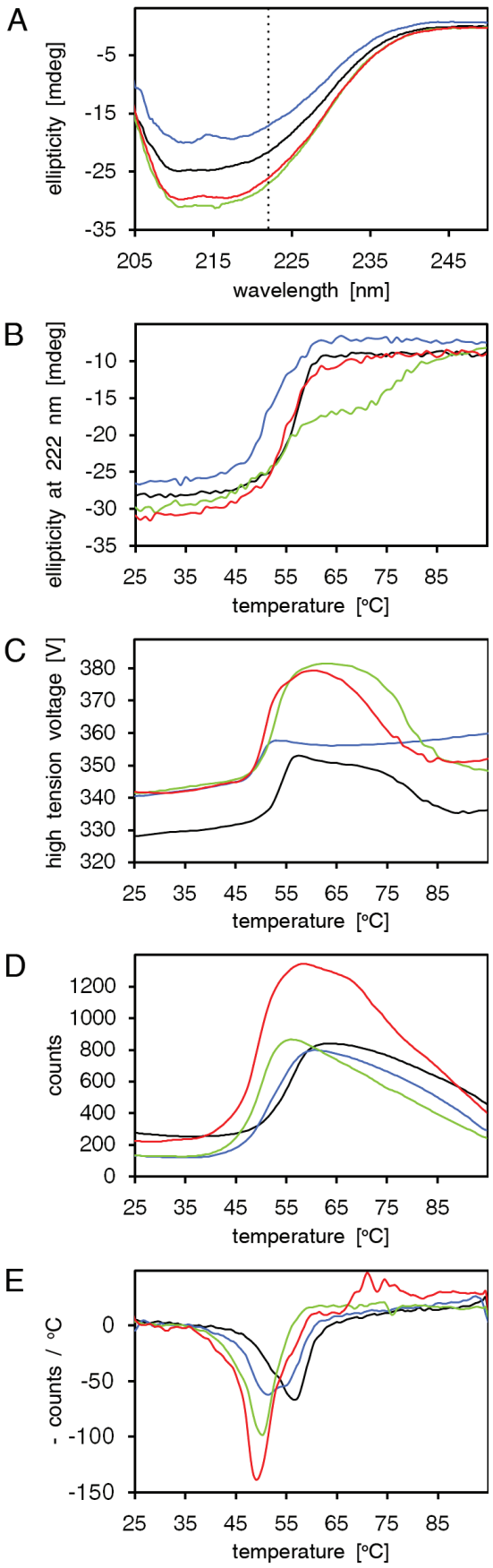

Results obtained at various pH values are reported in the Results and Discussion section. We performed similar experiments in the presence of various additives (NaCl, chaotropes, ethylene glycol). The results are summarized in Table S1. They support the observations made during experiments at various pH. Additional conclusions related to the role of ionic and hydrophobic interactions can also be drawn.

In general, chaotropes destabilize the enzyme, which can be seen by lower values of T_i. High ionic strength (addition of NaCl) does not seem to alter lipase properties much; all the parameters are similar to the ones measured without salt. This indicates that ionic interactions, which play a vital role in protein aggregation at acidic pH[S4], do not seem to affect the evolved mutants at neutral pH. However, in the other study certain thermostable mutants are sensitive to high salt concentration[S5].

Oppositely, thermal inactivation profiles revealed the significance of ionic interactions for activity retention. However, all differences in thermal inactivation profiles occur above Ti values determined using CD melting experiments. Therefore the raise of the maximum temperature where activity is fully retained in the presence of NaCl (as observed for all variants - except variant X - in thermal inactivation profiles) indicates that salts actually do not stabilize the native fold. Instead, high ionic strength rather facilitates re-constitution (possibly by preventing aggregation and/or precipitation) from early unfolding intermediates. This in turn suggests that initial unfolding processes are related exclusively to the reversible disruption of salt bridges. When these bridges are severely altered, as is the case for variant X, the re-constitution efficiency from early intermediates is limited.

Surprisingly, no melting and precipitation was observed for evolved mutants in ethylene glycol, contrary to the WT LipA case. This indicates that secondary structures remain intact even at high temperature

Figure S4. Example of Lipase A melting studies in 10 mM sodium phosphate, pH 7.0. Black curves represent data obtained for wild-type enzyme, blue corresponds to variant IX, green to variant X and red to variant XI. (A) Far-UV CD spectra. Dotted line indicates wavelength used to follow protein melting, 222 nm. (B) CD melting curves recorded at 222 nm wavelength. (C) CD high tension voltage curves recorded at 222 nm wavelength during melting experiments shown in panel B. (D) Fluorescence melting curves recorded using SYPRO Orange Protein Gel Stain as a hydrophobic fluorescent dye. (E) Negative temperature differential of fluorescence intensity vs. temperature derived from data presented in panel D.

		reference	50% ethylene glycol	95% ethylene glycol	2 M urea	4 M urea	1 M NaCl	1 M guanidinium hydrochloride
T_i [°C]	wild-type	51.8	50.8	38.1	39.6	26.3	53.6	37.4
	variant IX	45.6	41.3	n. d.	32.0	24.9	49.2	34.3
	variant X	48.5	41.9	n. d.	33.1	24.0	49.3	30.7
	variant XI	49.3	44.0	n. d.	34.3	25.4	48.6	30.8
slope [deg*cm^2/(mmol*K)]	wild-type	8.2	3.4	1.7	3.9	3.5	9.2	4.6
	variant IX	5.7	2.5	n. d.	3.3	2.6	6.8	5.0
	variant X	4.6	2.2	n. d.	4.6	2.1	7.8	3.9
	variant XI	6.0	2.8	n. d.	3.9	3.0	6.0	3.9
precipitation	wild-type	+	-	+	-	-	+	-
	variant IX	+	-	-	-	-	+	-
	variant X	+	-	-	-	-	+	-
	variant XI	+	-	-	-	-	+	-

Table S1. CD parameters determined for Lipase A variants in the solutions containing additives. The additives were combined with 10 mM sodium phosphate, pH 7.0 and 0.03% sodium azide (buffer used as a reference). The only exception was 95% ethylene glycol, which did not contain the buffer. In the panel describing protein precipitation, "+" means that protein precipitation was observed upon melting, whereas "-" indicates that no such process was observed.

in a more hydrophobic environment. Possibly, replacing intermolecular hydrophobic protein-protein interactions with protein-solvent interactions stabilizes secondary structures of LipA. However, the lack of activity retention of all LipA variants at high temperature (in thermal inactivation profile experiments) suggests that tertiary structure of the mutant is irreversibly altered upon heating in ethylene glycol. It can be associated to perturbations of hydrophobic core formation caused by solvent competing with protein.

It seems that a 1:1 mixture of ethylene glycol and buffer (pH 7) destabilizes the protein, since T_i values are lower than for the corresponding aqueous solution at pH 7. In contrast to our account, addition of polyhydroxyl alcohols was found to stabilize LipA according to Tm measurements, although generally this effect is less pronounced at neutral pH (7.8) in the presence of 60% ethylene glycol used in the study[S6].

Activity towards various substrates

Catalytic properties may be altered during the multiple rounds of directed evolution either due to proximity of the mutated residues to the binding and/or processing site, or due to allosteric effects. During the B-FIT study, residues 112, 134, 139 and 157 were mutated. All these residues are located in the proximity of the LipA active center[S7]. Therefore we decided to determine whether the substrate specificity had been affected. To achieve this goal, we determined the reaction rates under different hydrolytic conditions in the heterogeneous systems using mixtures containing Triton X-100 micelles harboring p-nitrophenyl esters with various unbranched acyl chain lengths [S8,S9] (Fig. S5), and also in homogeneous systems (Fig. S6). Activity in the homogenous setup was determined using water soluble substrates (*p*-nitrophenyl acetate, propionate and butyrate[S10]) without Triton X-100.

Experimental procedure

The reaction mixture consisted of: 20 µL of 4 to 40 µg/mL LipA variant in 10 mM sodium phosphate, pH 7.0, 0.03% sodium azide buffer; 5 µL of 100 mM substrate (*p*-nitophenyl ester) in acetonitrile and 175 µL of appropriate buffer. Mixtures were placed in a Nunc 96 Well Optical Bottom Plate (ThermoFisher Scientific). Reaction progress was followed colorimetrically

at 405 nm wavelength using a Spectramax Plus plate reader (Molecular Devices). The following *p*-nitrophenyl esters were studied: acetate, propionate, butyrate, caprylate and laurate. Reaction rates were determined in the following buffers: 50 mM potassium phosphate, pH 8.0; 50 mM glycine, pH 10.0; 50 mM potassium

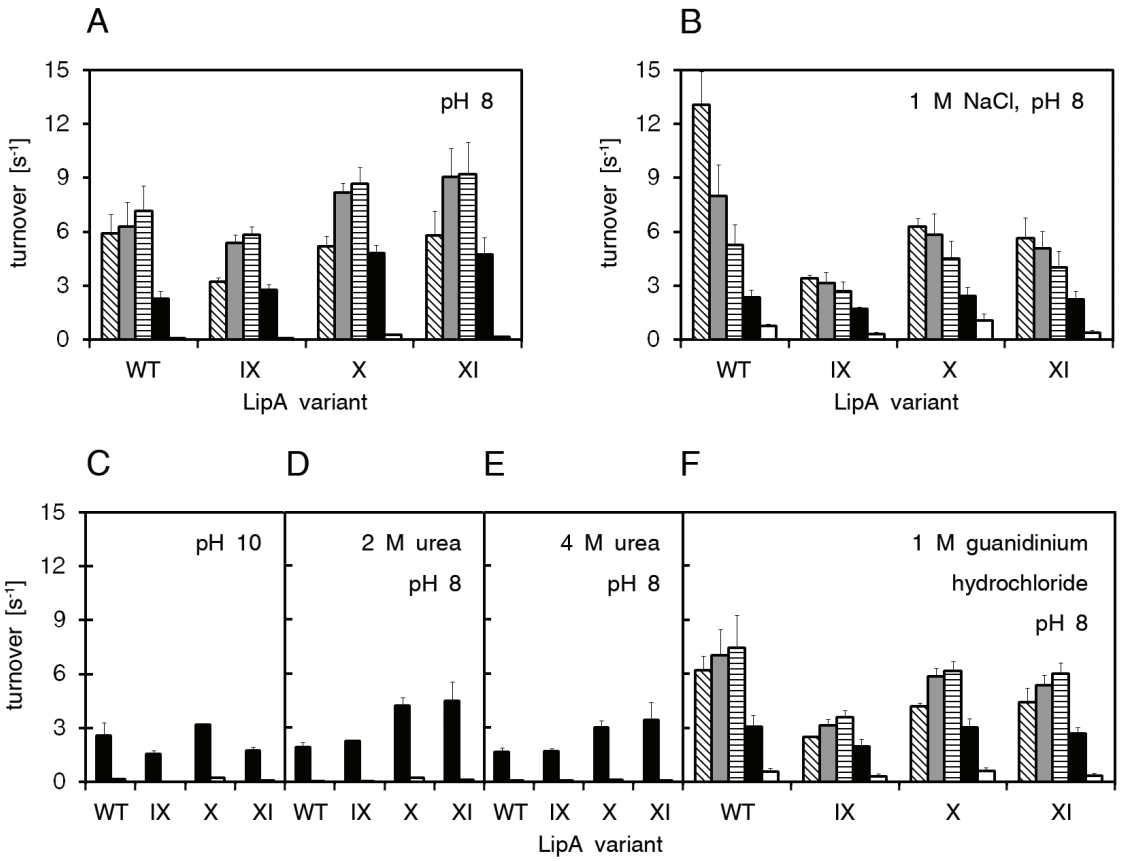

Figure S5. Rates of product formation in the heterogeneous hydrolysis of *p*-nitrophenyl esters catalyzed by LipA variants in the presence of Triton X-100. Bars with diagonal stripes correspond to hydrolysis rates determined for *p*-nitrophenyl acetate (two carbon atoms in the acyl moiety; C_2), gray bars to *p*-nitrophenyl propionate (C_3), bars with horizontal stripes to *p*-nitrophenyl butyrate (C_4), black bars to *p*-nitrophenyl caprylate (C_8), and white bars to *p*-nitrophenyl laurate (C_{12}).

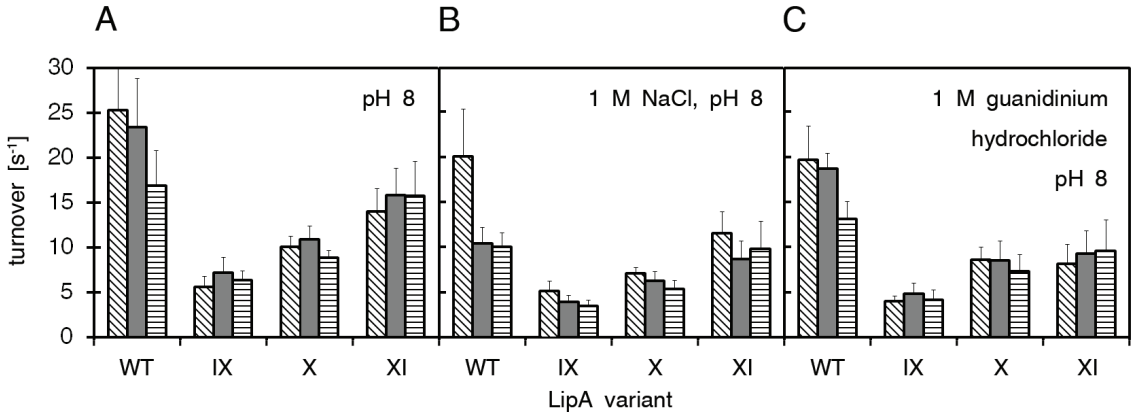

Figure S6. Rates of product formation in the homogeneous hydrolysis of *p*-nitrophenyl esters catalyzed by Lipase A variants. Black bars correspond to hydrolysis rates determined for *p*-nitrophenyl acetate, blue bars to *p*-nitrophenyl propionate and red bars to *p*-nitrophenyl butyrate.

phosphate, pH 8.0 with 1 M NaCl; 50 mM potassium phosphate, pH 8.0 with 2 M urea; 50 mM potassium phosphate, pH 8.0 with 4 M urea; 50 mM potassium phosphate, pH 8.0 with 1 M guanidinium hydrochloride. All buffers included 0.1% Triton X-100 for all substrates. Reaction rates for the soluble substrates (*p*-nitrophenyl acetate, propionate and butyrate) were determined using buffers without Triton X-100. All buffers contained 0.03% sodium azide. To determine turnover values, absorption coefficients of *p*-nitrophenol were determined for all of the reaction conditions.

Results

At pH 8 (Fig. S5A), i.e. under the original conditions used for screening during the directed evolution study[S1,S2], all LipA mutants exhibit a similar lipase activity profile towards the tested substrates. Overall, WT LipA and variant IX are slightly less active than variants X and XI, and the profile of WT indicates a higher activity towards *p*-nitrophenyl acetate relative to the more hydrophobic substrates than was found for the evolved mutants. Clearly, variants X and XI are more active towards *p*-nitrophenyl caprylate (a substrate used for screening purposes) than WT enzyme at the conditions used for screening. This could have been expected, as mutants with highest activity after thermal denaturation were selected in each round.

Secondly, the presence of high ionic strength affects the LipA catalytic characteristics significantly (Fig. 5B and S5F), although the relative activities towards the various substrates are similar for the different mutants. Once again, WT LipA deviates distinctly by having a higher activity towards *p*-nitrophenyl acetate.

The enzymatic hydrolysis of *p*-nitrophenyl caprylate by the evolved mutants proceeds slower at basic pH (Fig. S5C) than at pH 8, but not significantly different from WT LipA. Interestingly, 2 M urea does not affect lipase reaction rates significantly (Fig. S5D), and 4 M urea (sub-denaturing conditions, Fig. S5E) inhibits them only slightly.

The presence of high ionic strength (NaCl or guanidinium hydrochloride) affects reaction rates significantly. The rate of hydrolysis is inhibited by the presence of salts in both homogeneous and heterogeneous assays (Figs. S5B, S5F, S6B, S6C). Surprisingly, a high salt content promotes the hydrolysis of *p*-nitrophenyl laurate by all Lipase A variants in comparison to other conditions.

The result of the directed evolution is determined by the methods used to create evolutionary pressure, and the screening setup seems to be a vital factor. The results of our evolutionary study explicitly confirm this principle. The catalytic differences between WT and mutants may result from using a non-natural substrate for screening, as nature usually optimizes enzymes towards certain substrates. In vitro directed evolution would less likely change catalytic properties if the natural substrate were to be used. However, the unnatural substrate was chosen for practical reasons, and the different catalytic properties of the mutants are a consequence of this choice. The proximity of K112D, M134D, Y139C and I157M mutations (present in all studied mutants) to the catalytic site may underlie the catalytic differences between WT and mutants at the molecular level. The differences among variants IX, X and XI appear at positions 33-35, which are remote from the active site. Therefore relative activities toward various substrates are similar among these mutants.

Additionally, it was observed that the evolved mutants after heating at 80 °C and renaturation exhibit relative activity patterns toward the different substrates similar to the native variants, which confirms similar properties of native and thermally treated mutants.

Molecular dynamics simulations of Lipase A unfolding

Our experiments indicate that folding and aggregation properties of LipA are responsible for activity retention. Whereas experimental techniques like thermal inactivation profiles and CD probe protein properties, molecular dynamics (MD) is able to simulate the unfolding process and to suggest “hot-spots” on the molecular level, thus enabling correlation of experimental results not only with a static structural model, but also with dynamic processes.

The unfolding process of Lipase A was simulated using molecular dynamics performed at high temperature. The Desmond Molecular Dynamics System (D. E. Shaw Research[S11]) within the Maestro suite (Schrodinger, LLC) was used as a simulation tool. Four simulations were run for wild-type protein using structures deposited in Protein Data Bank under code 1I6W[S12], 1ISP[S13], 2QXT (chain A)[S4], 2QXU (chain A)[S4]. Another two simulations were run for variant X Lipase A using two models obtained during X-ray structure determination. All simulations were run at 500 K and analogous control simulations were performed at 300 K.

Computation settings: the protein molecule was simulated in a cubic water box with a solvent layer of 10 Å, 0.15 M NaCl ionic strength was used. The system was relaxed at 300 K or 500K and 1 atm prior to the simulation using NPT protocol with Berendsen thermostat and barostat. Simulation was run for 2 ns with recording interval 1.2 ps. An OPLS-2005 force field and SPC solvent model were used. NPT ensemble class at 1 atm pressure and 300 or 500 K was maintained using

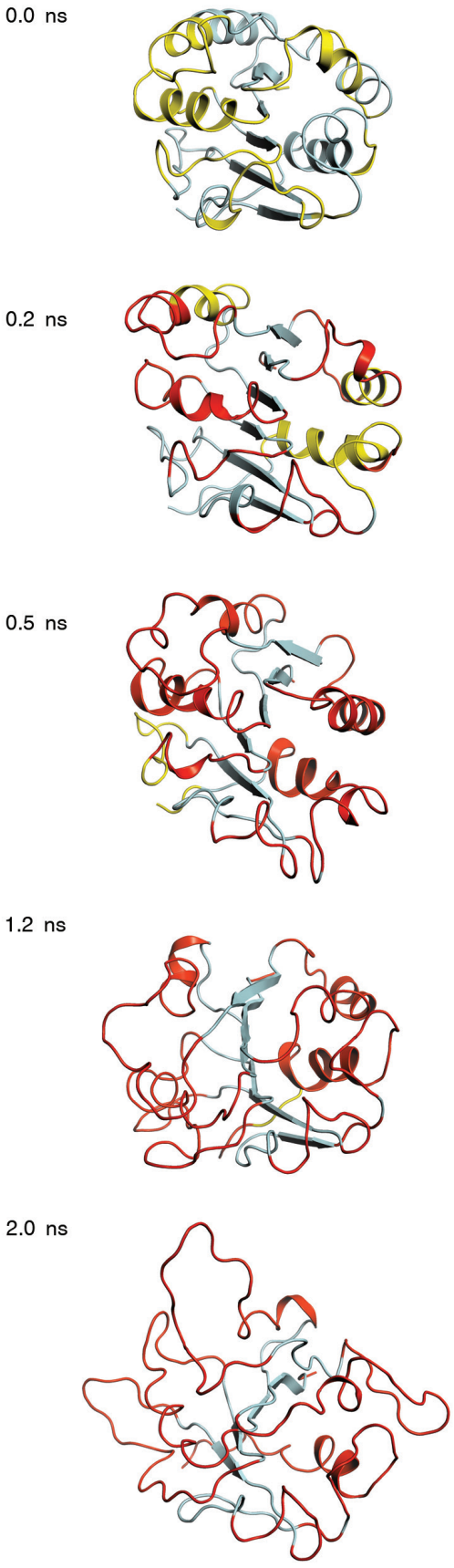

Figure S7. Molecular dynamics simulation of wild-type Lipase A melting at 500 K (chain A of PDB deposition 2QXT is shown as an example here). Snapshots taken at various time points of simulation as specified for each structure. Light blue-colored fragments of the molecule appear intact at the given time point. Yellow-color indicates fragments whose conformation will change between the given simulation time and the subsequent time point represented here. Red color indicates LipA fragments that have already melted prior to the given simulation time.

Martyna–Tobias–Klein barostat and Nose–Hoover thermostat. Coulombic interaction energies were computed using smooth particle mesh Ewald summation, where short range interactions were truncated at 9 Å. Interaction energies were integrated using RESPA with 2 fs time steps for bonded and short-range interactions, and 6 fs for long-range interactions.

Results were analyzed using MOLMOL[S14] and VMD[S15]. PyMOL (DeLano Scientific LLC) was used to prepare figures.

The MD computations performed in this study simulate the pattern of LipA melting. Fig. S7 features the time evolution of conformational changes during the simulation. Fig. S8 indicates the stability of various LipA fragments as simulated. It can be seen that the helical structures dislocate during the simulation, whereas β-strands do not seem to be severely affected. Helical structures occupy the periphery of the protein forming the lipase surface, and therefore they are exposed to solvent and are more prone to changes during simulations at high temperature. Strands form the core of LipA and due to limited accessibility to the solvent, they do not melt within 2 ns of simulation at 500 K. Comparison of the MD trajectories obtained for WT LipA and variant X did not reveal any significant differences on the tertiary structure level, i.e., the pattern of thermal unfolding is similar in both cases.

References

S1. Reetz MT, Carballeira JD, Vogel A (2006) Iterative saturation mutagenesis on the basis of B factors as a strategy for increasing protein thermostability. Angew Chem Int Ed Engl. 45:7745-7751.

S2. Reetz MT, Carballeira JD (2007) Iterative saturation mutagenesis (ISM) for rapid directed evolution of functional enzymes. Nat Protoc. 2:891-903.

S3. Hawe A, Sutter M, Jiskoot W (2008) Extrinsic fluorescent dyes as tools for protein characterization. Pharm Res. 25:1489-1499.

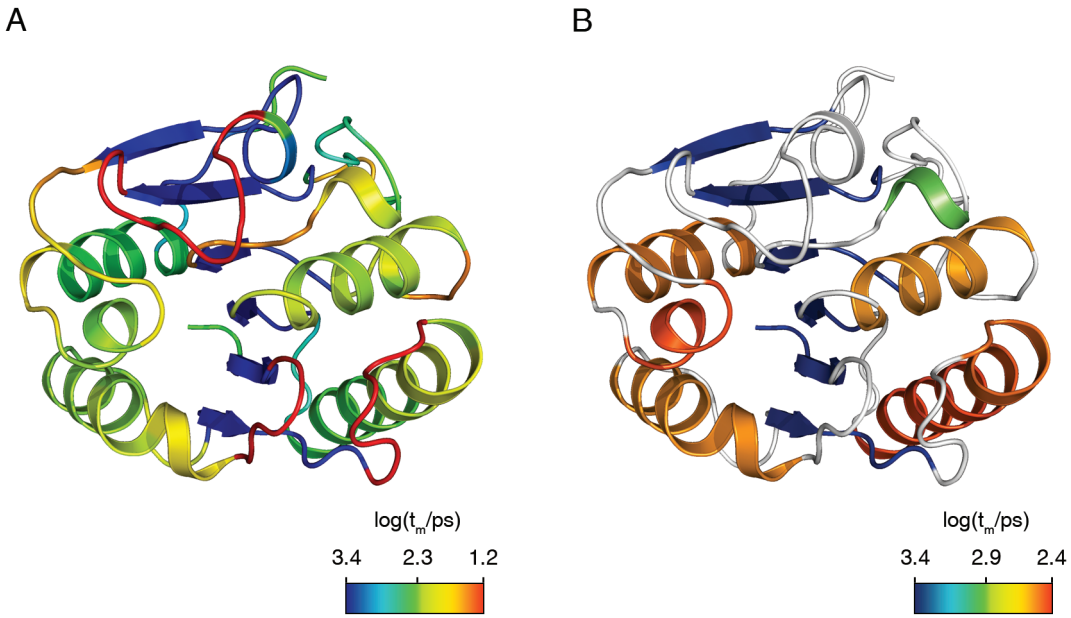

Figure S8. Relative stability of LipA fragments indicated by the time when the conformation of a given protein fragment changes significantly during simulation. The color spectrum reflects the time in a logarithmic scale. (A) Decay of native tertiary contacts within time. (B) Stability of each secondary structure.

S4. Rajakumara E, Acharya P, Ahmad S, Sankaranaryanan R, Rao NM (2008) Structural basis for the remarkable stability of Bacillus subtilis lipase (Lip A) at low pH. Biochim Biophys Acta. 1784:302-311.

S5. Ahmad S, Rao NM (2009) Thermally denatured state determines refolding in lipase: mutational analysis. Prot Sci. 18:1183-1196.

S6. Kamal MZ, Ahmad S, Rao NM (2011) Stabilizing effect of polyols is sensitive to inherent stability of protein. Biophys Chem. 156:68-71.

S7. Droge MJ, Boersma YL, van Pouderoyen G, Vrenken TE, Ruggeberg CJ, Reetz MT, Dijkstra BW, Quax WJ (2006) Directed evolution of Bacillus subtilis lipase A by use of enantiomeric phosphonate inhibitors: crystal structures and phage display selection. ChemBioChem. 7:149-157.

S8. Burdette RA, Quinn DM (1986) Interfacial reaction dynamics and acyl-enzyme mechanism for lipoprotein lipase-catalyzed hydrolysis of lipid p-nitrophenyl esters. J Biol Chem. 261:12016-1202.

S9. Redondo O, Herrero A, Bello JF, Roig MG, Calvo MV, Plou FJ, Burguillo FJ (1995) Comparative kinetic study of lipases A and B from Candida rugosa in the hydrolysis of lipid p-nitrophenyl esters in mixed micelles with Triton X-100. Biochim Biophys Acta. 1243:15-24.

S10. Ostdal H, Andersen HJ (1996) Non-enzymic protein induced hydrolysis of p-nitrophenyl acyl esters in relation to lipase/esterase assays. Food Chem. 55:55-61.

S11. Bowers KJ, Chow E, Xu H, Dror RO, Eastwood MP, Gregersen BA, Klepeis JL, Kolossvary I, Moraes MA, Sacerdoti FD, Salmon JK, Shan Y, Shaw DE, Scalable Algorithms for Molecular Dynamics Simulations on Commodity Clusters. In: (2006) Proceedings of the 2006 ACM/IEEE Conference on Supercomputing (SC06), Tampa, FL, 11 to 17 November 2006. ACM Press, New York.

S12. van Pouderoyen G, Eggert T, Jaeger KE, Dijkstra BW (2001) The crystal structure of Bacillus subtilis lipase: a minimal alpha/ beta hydrolase fold enzyme. J Mol Biol. 309:216-226.

S13. Kawasaki K, Kondo H, Suzuki M, Ohgiya S, Tsuda S (2002) Alternate conformations observed in catalytic serine of Bacillus subtilis lipase determined at 1.3 A resolution. Acta Crystallogr Sect D. 58:1168-1174.

S14. Koradi R, Billeter M, Wuthrich K (1996) MOLMOL: a program for display and analysis of macromolecular structures. J Mol Graphics. 14:51-55.

S15. Humphrey W, Dalke A, Schulten K (1996) VMD: visual molecular dynamics. J Mol Graphics. 14:33-38.